Acta Polytechnica CTU Proceedings **55**:63–70, 2025
https://doi.org/10.14311/APP.2025.55.0063

Published by the Czech Technical University in Prague

EXPERIMENTAL STUDY OF THE LEIDENFROST EFFECT IN THE CONTEXT OF HIGH HEAT FLUX COOLING

Vojtěch Smolík[a,*], Slavomír Entler[a,b], Pavel Zácha[a], Jan Podaný[a], Alžběta Endrychová[a], Marek Nejman[a]

[a] *Czech Technical University in Prague, Faculty of Mechanical Engineering, Department of Energetics, Technická 4, 160 00 Prague 6 – Dejvice, Czech Republic*

[b] *Czech Academy of Sciences, Institute of Plasma Physics, Za Slovankou 3, 182 21 Prague 8, Czech Republic*

[*] corresponding author: vojtech.smolik@fs.cvut.cz

Abstract. The behavior of water droplet on heated surfaces is experimentally observed to investigate the properties of the insulating vapor layer, a key element of the boiling crisis phenomenon. The lifetime of droplets on the heated surface is measured and compared with analytical models to examine the formation of the insulating vapor layer thickness between the coolant and the heated wall. The potential for reducing the Leidenfrost effect and increasing the critical heat flux by adjusting the surface roughness is examined to improve the thermohydraulic properties of the first-wall cooling channels. The behavior of water droplets on the heated surface with variable roughness is observed through the acoustic emission method. The behavior of water droplets on heated copper surfaces was experimentally studied using inductive and electrical heating with thermocouple temperature control, camera recording and acoustic emission analysis. The measured droplet lifetimes were compared with analytical models to evaluate the insulating vapor layer thickness. The practical relevance lies in reducing the Leidenfrost effect and increasing the critical heat flux, which can improve the cooling performance of high heat flux components such as tokamak first-wall channels.

Keywords: Leidenfrost effect, water droplet, evaporation, high heat flux cooling, boiling crisis, acoustic emission.

1. Introduction

The critical heat flux is an important parameter for designing water-cooled components of tokamak first wall. An insulating layer of vapor formed on the heated wall of the cooling channel above the critical heat flux is also a cornerstone of the Leidenfrost effect. The Leidenfrost effect (observed by Johann G. Leidenfrost [1]) is studied to improve the understanding of the insulating vapor layer between the liquid and the heated surface. In addition to the application in cooling channel design, previous researchers also studied this phenomenon in relation to spray cooling applications [2]. The similarity between the boiling crisis above the critical heat flux in the cooling channel and the Leidenfrost effect is shown in Figure 1.

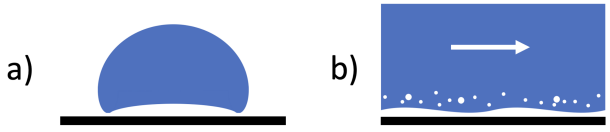

Figure 1. a) the Leidenfrost effect b) boiling crisis in cooling channel.

The geometry of Leidefrost droplets is dependent on the droplet radius. Small droplets have nearly spherical shape, droplets with radius greater than 1 mm obtain the typical Leidenfrost droplet shape shown in Figure 1a. The description of the Leidenfrost droplet shape in relation to its radius has also been a subject of study for many researchers [3, 4].

2. Method

Recent studies focused on the previously undescribed phenomenon of Leidenfrost droplet trampolining. It was observed that water drops will begin to oscillate and bounce on very smooth heated surfaces. The relation between heated surface rougness and Leidenfrost droplet trampolining was also examined in this experimental study [5–7].

Evaluating the evaporation time of a water droplet on a heated surface in relation to the surface temperature has been previously described in the literature by many researchers. Equations (1) to (5) are results of simplyfied analytical models found in the literature, which describe the mass and energy conservation of the Leidenfrost effect droplet. Biance (Equation (3)) adjusted the analytical model by experimentally measuring properties of the vapor film, thus it withstands among the other equations.

2.1. Analytical models

All analytical models evaluate the evaporation time of a droplet on the surface heated to a temperature above the Leidenfrost point.

Carey [8]:

$$\tau_{\text{evap}} = 1.21 \left[V_0 \left(\frac{\sigma}{\rho_l g} \right)^{-\frac{3}{2}} \right]^{\frac{5}{12}} \left(\frac{\rho_l^2 \mu_v h_u^3 \sigma^5}{\kappa_v^3 g^2 \rho_v \Delta T^3} \right)^{\frac{1}{4}}. \quad (1)$$

Zeuner [9]:

$$\tau_{\text{evap}} = \frac{4R_0^4}{5}\sqrt{6}\left[\frac{(K\Delta T)^3 \rho_v g}{\eta (L\rho_l)^3} \right]^{-\frac{1}{4}}. \quad (2)$$

Biance [10]:

$$\tau_{\text{evap}} = 2R_0^{\frac{1}{2}} \left[\frac{\sqrt{\frac{\sigma}{\Delta\rho_g}} 4\rho_l \lambda}{K\Delta T} \right]^{\frac{3}{4}} \left(\frac{3\eta}{\rho_v g} \right)^{\frac{1}{7}4}. \quad (3)$$

Maguet [11]:

$$\tau_{\text{evap}} = 4V_0^{\frac{1}{4}} \left(\frac{\rho_l \lambda}{K\Delta T} \right)^{\frac{3}{4}} \left[\frac{6\eta \left(\frac{2\pi R^2}{V_0} \right)^2}{\pi \rho_v g} \right]^{\frac{1}{4}}. \quad (4)$$

Mousa [12]:

$$\tau_{\text{evap}} = 0.725 \left(\frac{\eta \rho_l^3 \lambda^3 D_0^5}{g \rho_v K^3 \Delta T^3} \right)^{\frac{1}{4}}. \quad (5)$$

Lee [13]:

$$\lambda' = \lambda + \frac{1}{2} c_p \Delta T,$$

$$\frac{\rho_L R_0}{\tau_{\text{evap}}} = 1.1703 \cdot 10^{-2} \left(\frac{k\Delta T R_0 g \rho_V (\rho_L - \rho_V)}{\mu \lambda'} \right)^{\frac{1}{2}} + 2.3815 \left(\frac{\sigma \epsilon (T_p^4 - T_s^4)}{\lambda'} \right). \quad (6)$$

Two experimental approaches were used to examine the Leidenfrost effect. The first experimental setup is designed to achieve high temperatures of the heated plate to measure the evaporation time of water droplet on a wide range of temperatures. The second experimental measurements considered variable rougness of heated plates to examine the effect of surface roughness on the Leidenfrost effect. All of the experiments are performed using drops of distilled water and heated copper surfaces at atmospheric pressure.

2.2. Droplet evaporation time

The first experiment is focused on measuring the droplet evaporation time. Figure 2 shows a schematic of the experimental setup. The steel monoblock held by the ceramic insulation is heated by the inductive heating source. $12 \times 12 \times 2$ cm copper plate placed on a heated steel monoblock is used for experimental measurements. Water drops are placed on the heated copper surface using the FINNPIPETTE F2 10-100 µl

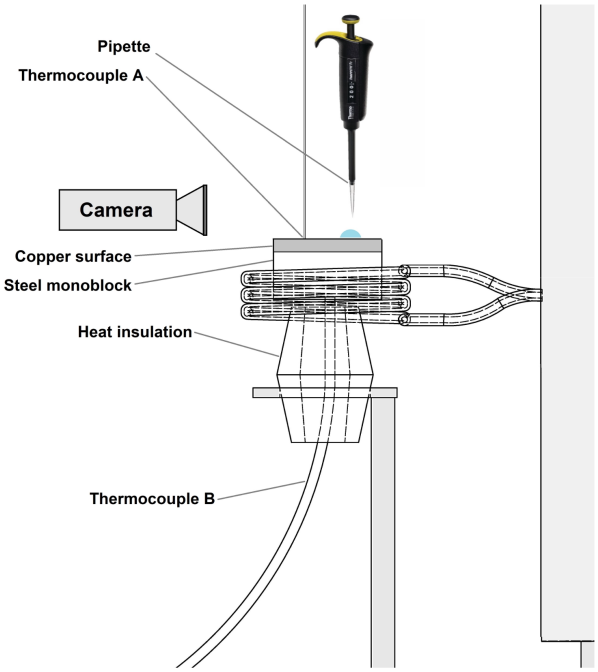

Figure 2. Experimental setup A with inductive heating.

Measuremd values	I.	II.	III.
Droplet volume V_0 [µl]	19	33	65
Volume uncertainty [µl]	±0.14	±0.15	±0.3
Droplet radius R_0 [mm]	≈ 1.65	≈ 2	≈ 2.5

Table 1. Droplet sizes used for measurements.

pipette, allowing the creation of an accurate drop volume for each measurement. Droplet volumes used for experimental measurements with the corresponding droplet radius and volume uncertainities of the pipette used are listed in Table 1.

Two thermocouples are attached to the experimental setup. Thermocouple A measures the temperature of the copper sufrace where the water drops are placed. Assuming that the temperature distribution through the copper block is symmetrical, the water droplets and the thermocouple A positions are located an equal distance from the center of the copper block. Thermocouple B is placed on the downside of the steel block and its measurements are used for the regulation of the induction heating source, thus a stable temperature is maintained for each measurement. The evaporation time of the water droplets is recorded by camera.

2.3. Surface roughness

The second experimental setup is shown in Figure 3. The water droplets are deposited on the heated surface by the automatic controlled valve located 2 cm above the heated plate. For this measurement, a set of six $2.5 \times 7 \times 1$ cm copper plates with variable surface roughness was manufactured. Copper samples were placed on the electric heater and each one was used

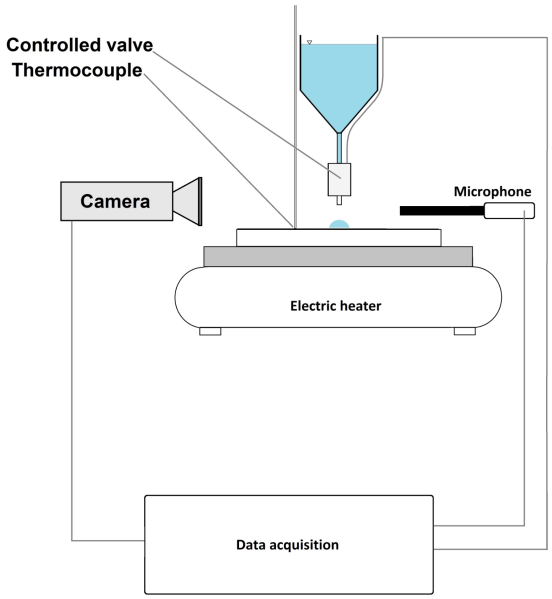

FIGURE 3. Experimental setup B with variable surface rougness.

Sample	Rz [µm]	± [µm]
A	1.92	0.21
B	2.14	1.04
C	2.28	0.30
D	2.88	0.92
E	2.92	0.71
F	1.86	0.45

TABLE 2. Surface roughness measurements (Rz values with uncertainties).

separately for the measurements. The thermocouple was attached directly to the copper plates next to the automatic valve.

The experimental setup is not designed to measure the evaporation time of the droplet but to observe the droplet behavior; thus, the copper plate samples are smaller in size than the previous setup. Surface roughness with corresponding uncertainities of manufactured samples is listed in Table 2 and Table 3. Samples A-E are also shown in Figure 4. The samples were manufactured by face milling and then processed with grinding and sanding to achieve variable surface roughness. Sample F was processed by metallographic polishing to achieve a very low roughness. All of the rougnesses are measured after a first set of trial tests was performed to take into account the surface rusting, an inevitable phenomenon in engineering applications. Microscopic surface profiles of selected samples are shown in Figures 5, 6 and 7. The automatic valve was controlled by Arduino to release drops of 1 mm in diameter when activated. The diameters of the droplets were adjusted by capturing the departing drops on camera. All measurements of the surface roughness effect on the Leidenfrost effect are performed on 2 mm diameter droplets.

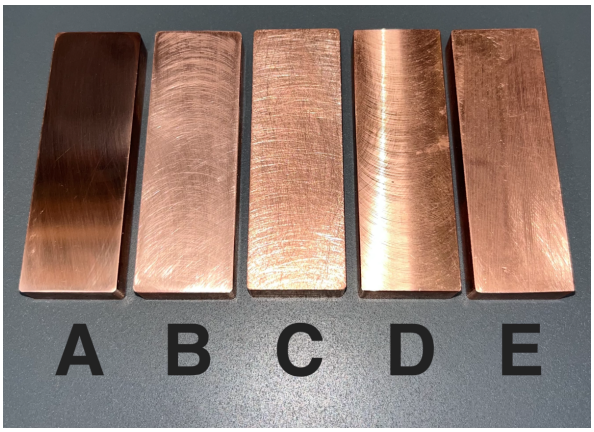

FIGURE 4. Experimental samples.

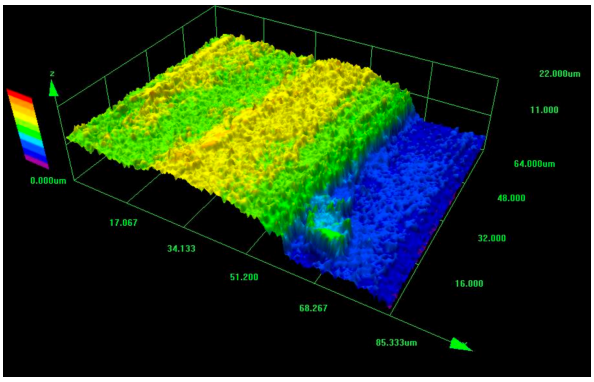

FIGURE 5. Sample D surface profile.

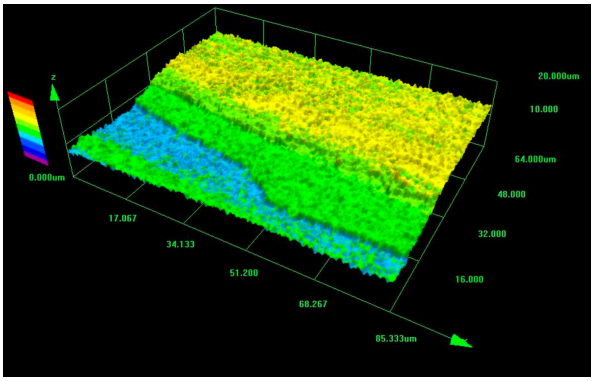

FIGURE 6. Sample B surface profile.

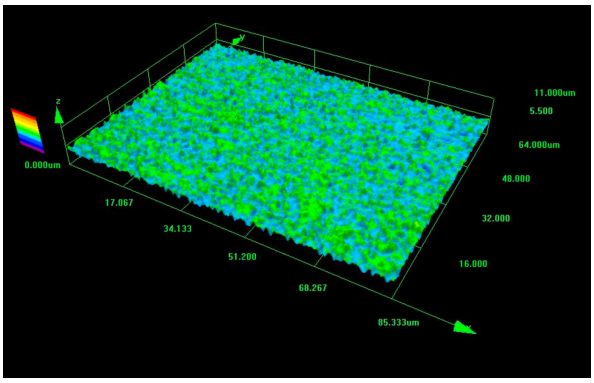

FIGURE 7. Sample F surface profile.

Sample	*Ra* [µm]	± [µm]
A	0.30	0.02
B	0.33	0.03
C	0.37	0.05
D	0.42	0.07
E	0.48	0.09
F	0.31	0.04

Table 3. Surface roughness measurements (Ra values with uncertainties).

Acoustic emission was used to evaluate the behavior of water droplets as an alternative to high-speed and high-resolution cameras often used by other researchers. The sounds of droplets in the regime of nuclete boiling, transition (bouncing) region, and the Leidenfrost region are clearly distinguishable. Acoustic emission recordings were processed by the SPEK v0.8.5 spectral analyzer; the resulting plots of acoustic analysis are presented. The thermocouple was attached to the surface of the experimental samples using a thermal paste, the expected accuracy of temperature measurements is ± 3 °C .

3. Results

The results of the droplet evaporation time measurement are presented in a form of equation describing the total evaporation time in relation to the surface temperature and initial droplet diameter. The surface rougness effect of the Leidenfrost effect was not focused on the evaporation time, but the measurements identified the borderline between the transition region defined by bouncing drops and the stable Leidenfrost effect through the acoustic emission analysis.

3.1. Droplet evaporation time

Figures 8, 9 and 10 show the results of experimental measurements of the droplet evaporation time in relation to the surface temperature for three different initial droplet volumes. The plots also show the predictions of evaporation time based on analytical models by previous researchers, described by Equations (1)–(5). Equation (6) from the work of Lee [13] is mentioned as a relevant contribution to the topic, but it was not used for the comparison, since its too complex. Experimental data clearly indicate that the evaporation time of water droplets increases rapidly when the surface temperature is 50 °C above the boiling point. The Leidenfrost point, defined by the longest evaporation time of the water droplet on the surface with a temperature above boiling point, is found around 110 °C above the boiling point for all measured droplet volumes.

The analytical models of previous researchers predict evaporation times longer than the experimental results observed. Biance model [10] is the only one that falls behind the experimental values and predicts shorter evaporation times than observed. The analytical model by Mousa [12] is the closest one to the experimental values, thus this model was corrected to fit the measured data, resulting in Equation (8).

The correction of the Mousa model is defined by $-20 \cdot \frac{\Delta T_{SL}}{\Delta T}$ in Equation (8). ΔT_{SL} is described by Equation (7), the result of the second part of this research, the borderline of the stable Leidenfrost effect in dependence on surface roughness.
For $1.8 \leq Rz\,[\mu m] \leq 3$:

$$\Delta T_{SL} = -64 \cdot Rz + 230. \tag{7}$$

For $\Delta T \geq \Delta T_{SL}$ and $D_0 \geq 1\,\mathrm{mm}$:

$$\tau_{\mathrm{evap}} = 0.725 \left(\frac{\eta \rho_l^3 \lambda^3 D_0^5}{g \rho_v K^3 \Delta T^3} \right)^{\frac{1}{4}} - 20 \cdot \frac{\Delta T_{SL}}{\Delta T}. \tag{8}$$

3.2. Surface roughness effect

A set of experimental samples with variable surface roughness was measured to examine its influence on the Leidenfrost effect. It was found that water drops bounce on a smooth heated surface on a broader range of temperatures compared to the rough surface. The state in which doplets stop bouncing and stay steadily on heated surfaces was named "the steady Leidenfrost effect". The steady Leidenfrost effect and transition region of bouncing droplets were distinguished by the acoustic emission method.

Figures 11, 12 and 13 show representative examples of three observed droplet states: rapid nucleate boiling, transition region with bouncing droplets, and the steady Leidenfrost effect. The transition region shown in Figure 12 is observed to achieve a constant bouncing frequency around 30 Hz. The absence of significant acoustic emission in the steady Leidenfrost effect (Figure 13) suggests a very low evaporation rate; therefore, the heat exhaust is lower compared to the transition region.

Acoustic emission spectral analysis – a visual representation of recorded sound shows the spectrum of sound frequencies (axis x) captured in time (axis y). The relative level of sound pressure measured in decibels (dB) is expressed by a color scale. It is assumed that the evaporation rate of the water droplet corresponds to the sound pressure level. Figures 11, 12 and 13 show the 2 second recordings of acoustic emission for three representative stages of the droplet on a heated surface of sample F with surface rougness of 1.86 µm Rz.

Figure 14 shows the results of the experimental measurements. Each sample was tested repeatedly to find a borderline between the transition region and the steady Leidenfrost effect. The mean values of the borderline temperature were processed by least-squares analysis to find a linear function that describes the relation between surface roughness and borderline temperature, resulting in Equation (7). The borderline between nucleate boiling and the transition region

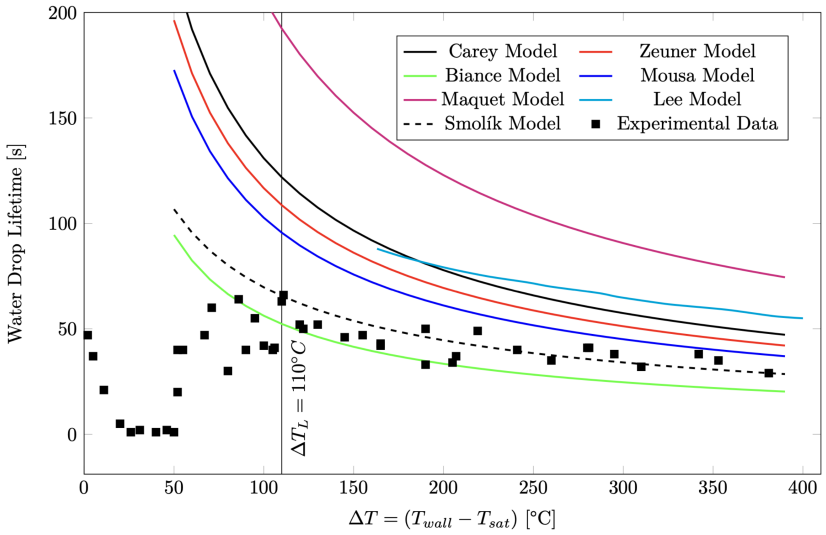

FIGURE 8. Evaporation time,$V_0 = 19\,\mu l$, $R_0 = 1.65\,mm$.

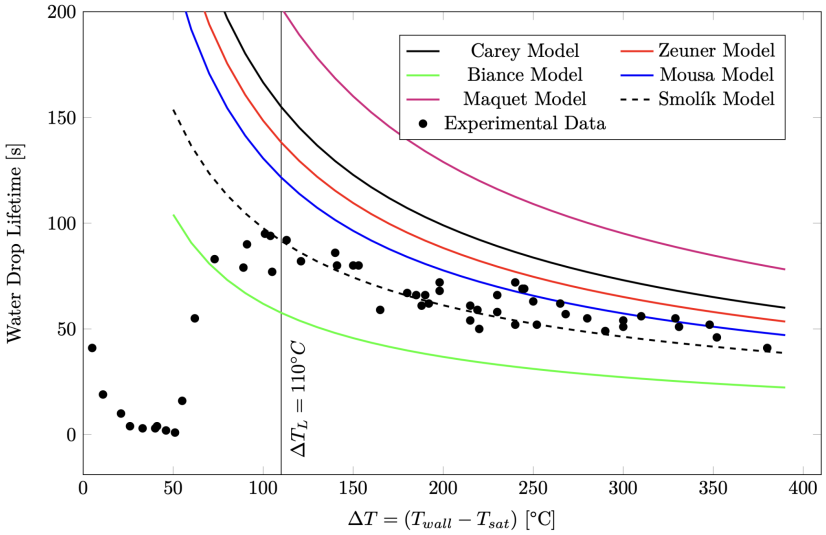

FIGURE 9. Evaporation time, $V_0 = 33\,\mu l$, $R_0 = 2\,mm$.

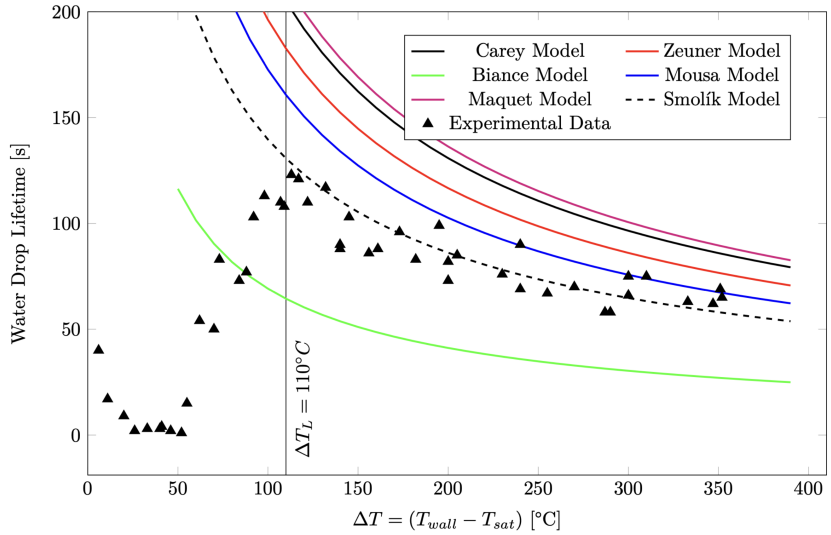

FIGURE 10. Evaporation time, $V_0 = 65\,\mu l$, $R_0 = 2.5\,mm$.

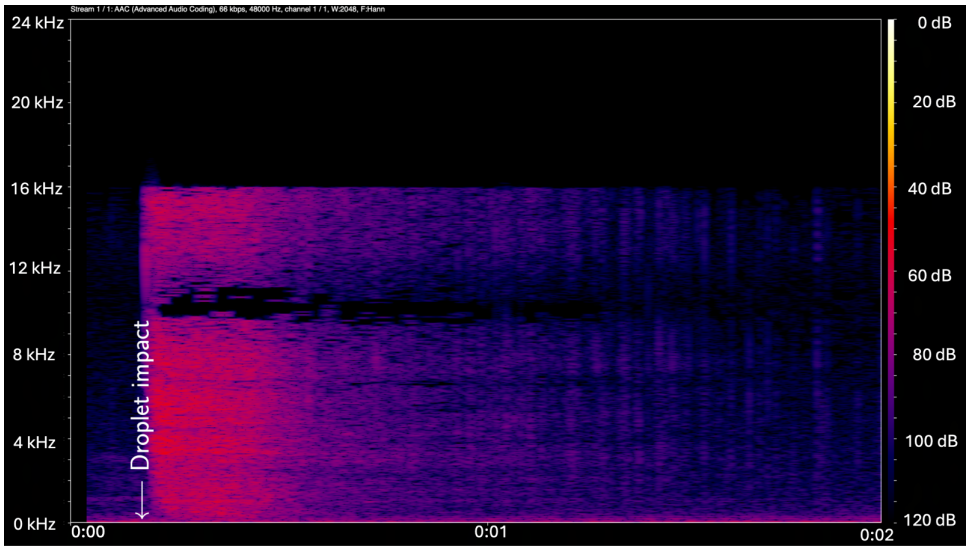

Figure 11. Nucleate boiling acoustic emission, dT = 10 °C.

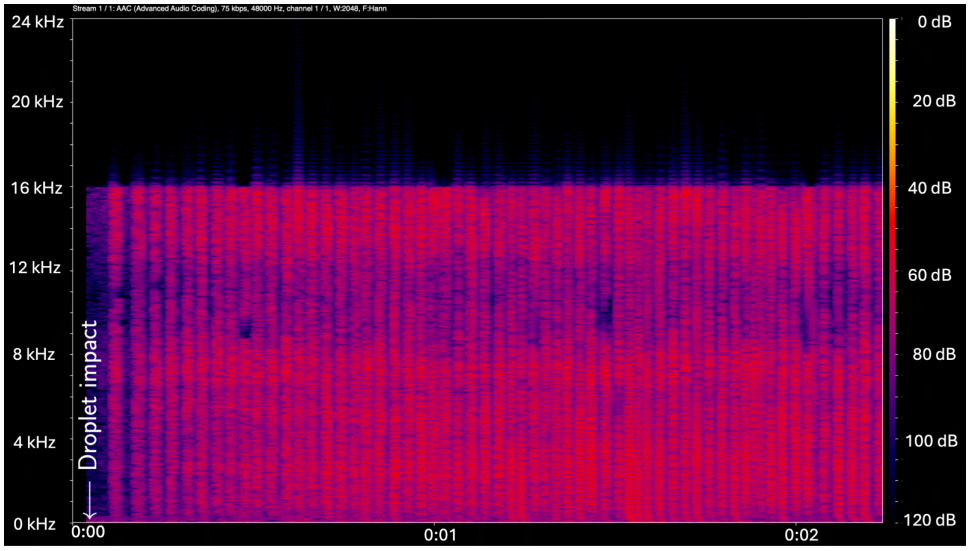

Figure 12. Transition region (bouncing) acoustic emission, dT = 100 °C.

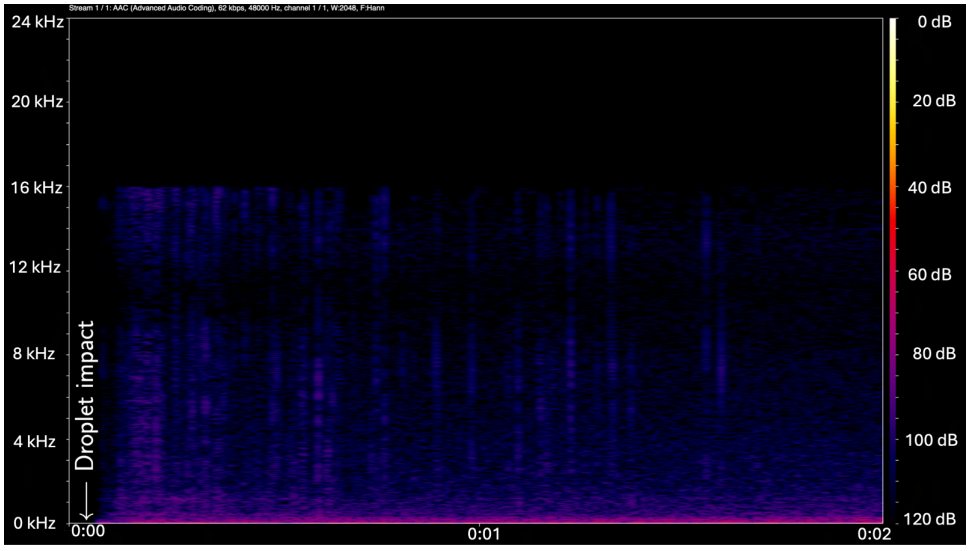

Figure 13. Leidenfrost effect acoustic emission, dT = 120 °C.

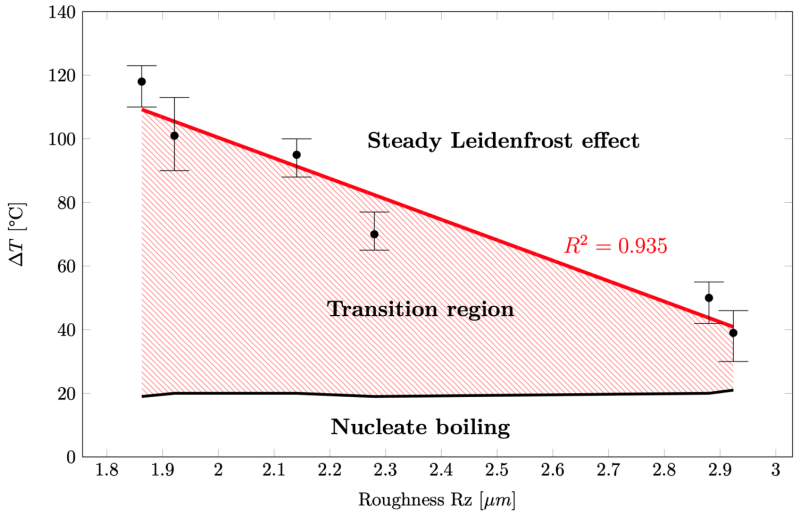

FIGURE 14. Regions of the Leidenfrost effect in relation to surface roughness.

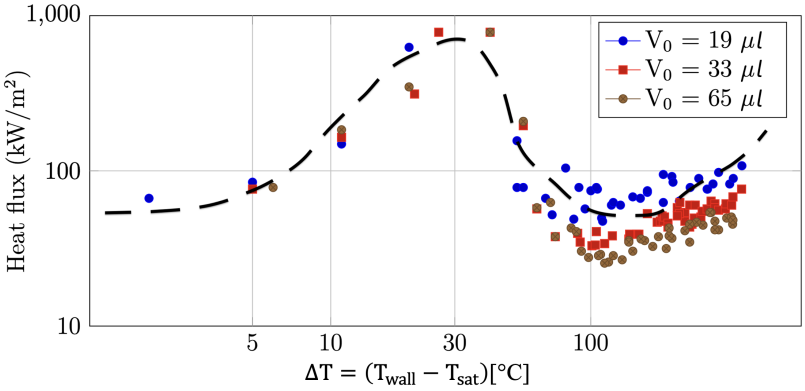

FIGURE 15. Nukiyama's boiling curve observed on the Leidenfrost effect.

was found to be at a constant value of 20 °C above the boiling point.

3.3. NUKIYAMA'S BOILING CURVE

Experimental data shown in Figures 8, 9 and 10 can also be interpreted to show a relation between wall temperature and heat flux cooled by the evaporating droplet. For this purpose, a water droplet is simplified to a semisphere with a volume equal to the droplet volume found in experimental measurements. The radius of the sphere r_{evap} in Equation (9) defines the area through which all evaporated heat of the droplet is dissipated. Equation (10) represents the heat flux calculation used in the processing of results.

$$r_{\text{evap}} = \sqrt[3]{\frac{6 \cdot V_0}{4 \cdot \pi}}. \tag{9}$$

$$q_{\text{evap}} = \frac{E_{\text{evap}}}{T_{\text{evap}} \cdot A_{\text{evap}}} = \frac{V_0 \cdot \rho \cdot \lambda}{T_{\text{evap}} \cdot \pi \cdot r_{\text{evap}}^2}. \tag{10}$$

Figure 15 shows the experimental measurements of the Leidenfrost effect interpreted in relation to wall temperature and wall heat flux. The resulting plot shows the same characteristics as Nukiyama's boiling curve, clearly indicating there are multiple boiling regimes observable in a Leidenfrost droplet.

4. DISCUSSION

Analytical models of the Leidenfrost droplet evaporation time are very rarely validated by experimental data measured on a broad range of temperatures. This study provides an overview of existing models and comparison of experimental results and analytical predictions for three different initial droplet volumes on a broad scale of temperatures. Some previous researchers observed that ethanol droplets reduce the boiling point and extend the Leidenfrost region, and this study measured the properties of water droplets to provide more suitable data for engineering applications.

A recent study by G. Graeber [5] suggested that the bouncing of Leidenfrost droplets is not a consequence of initial droplet impact, but an outcome of the naturally occurring oscillation of droplets in the Leidenfrost state. Water droplets in this research were released 2 cm above the heated surface, as it is necessary to build an aluminum foil thermal insulation around the automatic valve releasing the droplets. However, releasing the droplets manually directly onto the heated surfaces did not result in significant changes in the observed phenomenon.

5. Conclusion

In the first part of this study, the evaporation time of three different droplet volumes was measured on a broad range of surface temperatures. All of the experimental measurements considered copper surface samples and distilled water droplets. An existing analytical model of the Leidenfrost droplet evaporation time was adjusted to fit the experimental data, resulting in Equation (8).

The second part of this study examined the relationship between surface roughness and the Leidenfrost effect. Bouncing and trampolining of droplets on the heated surface was defined as the transition region. The state in which the droplet stays on the heated surface without any disturbance is defined as stable Leidenfrost effect. The borderline temperature between the transition region and the stable Leidenfrost effect was observed through the acoustic emission method and was found to be strictly dependent on the surface roughness. The borderline stable Leidenfrost effect temperature of smooth surfaces is observed to be significantly higher than on rough surfaces. The resulting relation of this effect is expressed in Equation (7).

The Nukiyama boiling curve was extracted from the Leidenfrost droplet evaporation measurements to prove there are multiple boiling regimes observable in a single droplet, similar to the pool boiling regimes.

List of symbols

ϱ Density [$\mathrm{kg\,m^{-3}}$]
μ Viscosity [$\mathrm{Pa\,s}$]
c_p Specific heat [$\mathrm{J\,kg^{-1}\,K^{-1}}$]
D_0 Initial drop diameter [m]
h_l Heat of vaporization [$\mathrm{J\,kg^{-1}}$]
g Gravity acceleration [$\mathrm{m\,s^{-2}}$]
K Thermal conductivity [$\mathrm{W\,m^{-1}\,K^{-1}}$]
l_c Capillary length [m]
R_0 Initial drop radius [m]
T Temperature [K, °C]
V_0 Initial drop volume [$\mathrm{m^3}$]
ϵ Emissivity [–]
λ Latent heat [$\mathrm{kJ\,kg^{-1}}$]
λ' Modified latent heat [$\mathrm{kJ\,kg^{-1}}$]
σ Surface tension [$\mathrm{N\,m^{-1}}$]
σ_{SB} Stefan-Boltzmann constant [$\mathrm{W\,m^{-2}\,K^{-4}}$]
τ_{evap} Evaporation time [s]

Subscripts:
l Liquid [–]
v Vapour [–]

Acknowledgements

This work was supported by: Student Grant Competition, Czech Technical University in Prague, SGS23/159/OHK2/3T/12.

References

[1] J. G. Leidenfrost. On the fixation of water in diverse fire. *International Journal of Heat and Mass Transfer* **9**(11):1153–1166, 1966. https://doi.org/10.1016/0017-9310(66)90111-6

[2] P. Kotrbacek, M. Chabicovsky. Influence of the surface roughness on the cooling intensity during spray cooling. In *Proceedings 25th Anniversary International Conference on Metallurgy and Materials*, pp. 41–46. 2019.

[3] I. Chakraborty, M. V. Chubynsky, J. E. Sprittles. Computational modelling of Leidenfrost drops. *Journal of Fluid Mechanics* **936**:A12, 2022. https://doi.org/10.1017/jfm.2022.66

[4] J. C. Burton, A. L. Sharpe, R. C. A. van der Veen, et al. Geometry of the vapor layer under a Leidenfrost drop. *Physical Review Letters* **109**(7):074301, 2012. https://doi.org/10.1103/PhysRevLett.109.074301

[5] G. Graeber, K. Regulagadda, P. Hodel, et al. Leidenfrost droplet trampolining. *Nature Communications* **12**(1):1727, 2021. https://doi.org/10.1038/s41467-021-21981-z

[6] P. Agrawal, S. Dash. Droplet trampolining on heated surfaces in the transitional boiling regime. *International Journal of Heat and Mass Transfer* **190**:122811, 2022. https://doi.org/10.1016/j.ijheatmasstransfer.2022.122811

[7] D. Liu, T. Tran. Leidenfrost droplets trampoline. arXiv:1912.10744, 2019. Preprint on arXiv. https://doi.org/10.48550/arXiv.1912.10744

[8] V. P. Carey. *Liquid-Vapor Phase-Change Phenomena.* Hemisphere Pub. Corp., Washington, D.C., 1992.

[9] M. Zeuner, K. Schwark, C. Hanisch, M. Ziese. Leidenfrost effect studied by video analysis. *European Journal of Physics* **40**(6):065101, 2019. https://doi.org/10.1088/1361-6404/ab37d6

[10] A.-L. Biance, C. Clanet, D. Quéré. Leidenfrost drops. *Physics of Fluids* **15**:1632–1637, 2003. https://doi.org/10.1063/1.1572161

[11] L. Maquet. *Leidenfrost effect at its limits.* Ph.D. thesis, Université Libre de Bruxelles, Ecole Polytechnique, Bruxelles, France, 2017.

[12] M. Mousa. Droplet evaporation time in film boiling region. *Alexandria Engineering Journal* **38**(4):241–252, 1999. [2025-09-10]. https://eng.alexu.edu.eg/images/Alex-Eng-Journal/Volume_38-1999/Volume_38-no.4/Droplet_Evaporation_Time_In_Film_Boiling_Region.pdf

[13] C. J. Lee. *A Theoretical and Experimental Investigation of The Leidenfrost Phenomenon for Small Droplets.* Ph.D. thesis, Oklahoma State University, Stillwater, Oklahoma, USA, 1965.